ELSEVIER

Journal of Power Sources 66 (1997) 89–96

JOURNAL OF POWER SOURCES

Determination of internal resistance and electrocatalyst utilization of fuel cells

José A. Garcia *, C.A. Ward, R.D. Venter, S. Ho

Thermodynamics and Kinetics Laboratory, Mechanical Engineering Department, University of Toronto, Toronto, M5S 1A8, Canada

Received 25 January 1996; accepted 27 August 1996

Abstract

Analytical methods have been proposed recently for determining both the internal resistance of fuel cell electrodes and the fraction of the electrocatalyst that is completely utilized. To apply these methods requires that the Tafel slope and the equilibrium exchange current for the electrolyte–electrocatalyst combination to be known when this combination is exposed to O_2 and when it is exposed to H_2. The Tafel parameters have been previously reported for O_2 and their measurement for H_2 is reported herein. Also, to apply one of these analytical methods — maximum power method — requires that the current and potential to be measured when a fuel cell is operating at steady state and at maximum power. To apply the second method — approximate maximum power method — requires that the cell potential and slope of the potential versus current curve be measured at a current that is less than that corresponding to maximum power. To evaluate these methods, a series of porous carbon electrodes were constructed, and to give them different resistances nickel was electro-deposited on the one side of each. These electrodes were then assembled into fuel cells and tested. Their internal resistance was determined by the current-interrupt technique, and by using the analytical methods. These results agree to within the experimental error, 12%. Electro-depositing nickel on the gas side of the electrodes was found to decrease their internal resistance by an order of magnitude and increase the electrocatalyst utilization by a factor of three.

Keywords: Fuel cells; Internal resistance; Electrocatalyst utilization

1. Introduction

Several experimental and theoretical studies on the relation between electrochemical performance and physical properties of porous electrodes have been reported [1–13]. Some of the characteristics sought in such electrode structures are: (i) rapid diffusion of reactants to the electrode–electrolyte–gas interface; (ii) ready diffusion of products and non reactive diluents from the interface without limiting transport of reactants; (iii) a stable position of the electrode–electrolyte–gas interface; (iv) maximum effective catalytic area, and (v) minimum ohmic resistance. Herein the effect of these last two characteristics on the performance of the fuel cell is examined more carefully.

The internal resistance of a fuel cell is defined as the resistance measured through the electrolyte between the poles of the external load. The value of the internal resistance depends on the resistivity of several of the materials that are chosen to construct the fuel cell, on the design of the fuel cell, and the manufacturing of the electrodes. Since the fuel cell usually operates at a low voltage and high currents to generate useful amounts of power, significant losses can be present in a fuel cell due to its internal resistance.

The fraction of the electrocatalyst placed in the electrodes during the manufacturing process that is fully utilized during the operation of the fuel cell is another parameter that is particularly important in determining fuel cell performance. The electrocatalyst is usually dispersed as small particles on a carbon substrate and the catalyzed carbon is placed in the interior of the electrode near the current collector. The effectiveness of the electrocatalyst depends on both the properties of the electrocatalyst–electrolyte combination and on the manufacturing of the electrodes. Both parameters, can only be assessed once the electrodes have been assembled into a fuel cell and operated to produce power.

Recently analytical methods to determine both the internal resistance and the fraction of the electrocatalyst that is used effectively in a fuel cell have been proposed [14]. In order to apply the proposed methods, the electrokinetic parameters of the electrocatalyst–electrolyte combination have to be known. The electrokinetic parameters for oxygen reduction at a platinum–potasium hydroxide are available [15]. The

* Corresponding author.

PII S0378-7753(96)02486-X

rotating disk measurements of hydrogen oxidation at a platinum–potassium hydroxide (KOH) interface are reported herein. In order to evaluate these methods a series of porous carbon electrodes with different power production capacities were constructed. These electrodes were assembled into single fuel cells and tested. The internal resistance and effective catalyst fraction of these fuel cells were determined by the proposed methods. The estimated internal resistance was compared with that determined independently by the current interrupt technique. The experimental procedure for the rotating disk measurements and fuel cell tests as well as the discussion of the results are presented in the following sections.

2. Experimental

2.1. Electrokinetic parameters of hydrogen oxidation at a platinum–potassium hydroxide interface

The electrochemical oxidation of hydrogen at a platinum–potassium hydroxide (KOH) interface was studied using the rotating disk electrode (RDE). The experimental arrangement and procedure were similar to those reported in a previous study of the oxygen reduction for the same interface [15]. Experiments were carried out at three different concentrations of KOH: 0.1, 0.5 and 6.0 N, and at three different temperatures: 45, 65 and 80 °C. Ultra-pure potassium hydroxide was used in double-distilled organic free water. Solutions were prepared immediately before each experiment to insure purity. A jacketed glass cell was used to control the temperature. A dynamic hydrogen electrode (DHEL) with a lugging probe placed at approximately 1.0 cm below the disk was used as a reference electrode. The temperature of the cell was monitored by a thermocouple and was controlled by circulating heated water.

A Pine instrument's bipotentiostat (Model RDE3) was interfaced with a microcomputer. For all studies described here, a scanning rate of 10 mV/s was used. Cyclic voltammograms were recorded at a scan rate of 100 mV/s. A Pine Instrument's rotator (PIR) was used to rotate the Pine's Model DDT6 ring-disk electrode. The disk electrode had an apparent geometric electrode area of 0.456 cm^2 with its geometry of $r_1 = 0.382$ cm, $r_2 = 0.399$ cm, and $r_3 = 0.422$ cm, respectively. Here, r_1 is the radius of the disk electrode, and r_2 and r_3 are radii of inner and outer circles of the ring electrodes, respectively. Both disk and ring electrodes were made of platinum; the ring-disk electrodes were used as delivered. The electrodes were polished to a mirror finish with 1 μm aluminum powder. These electrodes were always cleaned overnight in chromic acid prior to each use, and were then rinsed with a copious amount of double-distilled water.

The electrolyte solution was purged with nitrogen gas for at least 30 min, then a cyclic voltammogram was recorded with a scan range of 0.03 to 1.2 V. This served as a check for the purity of the electrolyte solution as well as that of the electrode. The solution was then saturated with hydrogen gas for 2 h at room temperature. Then the temperature was brought to the desired level during the last hour of saturation. This would prevent the loss of moisture at higher temperatures. The rotating disk electrode was scanned at various rotating speeds: 500, 1000, 2000, 3000, 4000 and 5000 rpm. For each speed, six scans were performed.

2.2. Nickel coated carbon electrodes for alkaline fuel cells

The fuel cell electrode that we studied is of the multilayer type that utilizes platinum as the catalyst, Teflon™ as the binding agent, and porous carbon as the backing structure or substrate. Nickel is electrodeposited on the gas side of the porous carbon electrodes; the technique used for depositing the nickel is referred to as 'Electrochemical Metallizing' (Selectrons, Wartbury, CT, USA). This technique is basically a high current density electrochemical process for depositing metals on any conductive surface without the immersion of the part in a plating bath.

The substrate used for the manufacturing of all electrodes was a carbon paper (Stackpole PC 206, Stackpole Corporation, St. Marys, PA, USA). The porosity of the paper, as received from the manufacturer, was approximately 80%, its thickness ranged from 0.3 to 0.5 mm and its weight per geometric area was about 140 g/m^2. Teflon™ was used as the binding agent to provide the electrode with enhanced strength and wet proofing properties. This binding agent was an aqueous solution of fluorocarbon particles that contained 5 wt.% of a wetting agent (Photoflow™). The catalyst used in the electrodes was platinum; the average size of the platinum particles was 20 Å in diameter (as specified by the manufacturer, Prototech, Highlands, MA, USA) and previously deposited on carbon employing a ratio of 10 wt.% platinum.

The flow sheet of the manufacturing process of the electrodes is shown in Fig. 1. The carbon paper as received from the manufacturer was first water proofed with a mixture of 45 wt.% polytetrafluoroethylene (Teflon™). The water proofed paper was then dried at room temperature. The nickel coating was deposited on one side of the paper using the electrometallizing technique and then rinsed with distilled water. The diffusion layer was sprayed on the opposite side of the paper. The mixture used to spray this layer was made of carbon powder (SH-100), 30 wt.% Teflon™, 5 wt.% Photoflow™ and distilled water. Then a second layer that contained the activated carbon mixture (10 wt.% platinum), 25 wt.% Teflon™, 5 wt.% Photoflow™ and distilled water was deposited. A third layer being a repeat of the second layer except that the Teflon™ was reduced to 15 wt.% was then sprayed. Finally, the nickel coated carbon paper with the three sprayed layers were sintered at 330 °C and 15 kg/cm^2 for 10 min. The amount of platinum per unit area deposited in all electrodes was approximately 0.2 mg/cm^2. An schematic representation of the final electrode structure is shown in Fig. 2.

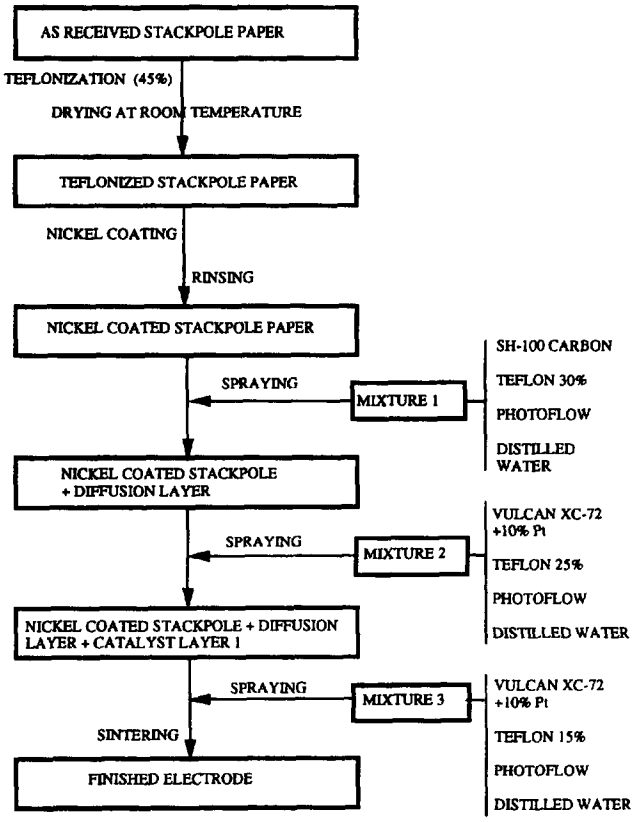

Fig. 1. Flowsheet for the manufacturing process of nickel coated electrodes.

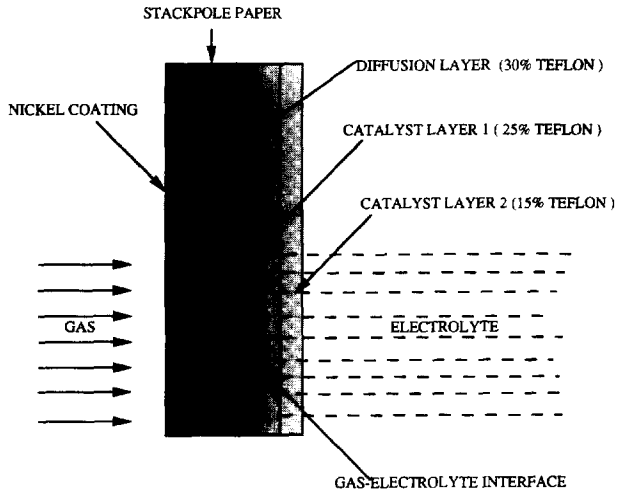

Fig. 2. Schematics of the structure of a nickel coated porous carbon electrode and its interface layer.

Depositing different amounts of nickel on the carbon substrate altered its ohmic resistance. A half-cell system having an area of 11.2 cm^2 and similar in construction to the unit reported in Ref. [16], was used for testing the performance of single electrodes. The square wave method [17] was used to determine the ohmic resistance of these electrodes.

Three sets of electrodes were prepared for performance and internal resistance measurements; the amount of nickel deposited on these sets of electrodes was 10, 19 and 29 mg/cm^2, respectively. The performance tests were carried out at temperatures of 26, 43 and 62 °C with each electrode tested as an anode (hydrogen electrode) and as a cathode (oxygen electrode). Once the electrochemical performance of the electrodes were determined, larger electrodes having a surface area of 64 cm^2 were manufactured and assembled in single fuel cells to study the effect of the internal resistance in their performance. The electrode separation in all four cells was 1.8 mm. The internal resistance measurements on these single fuel cells were carried out using the current interrupt method [19].

3. Results and discussion

3.1. Rotating disk electrode studies

A typical RDE voltammogram for 0.1 N, 65 °C and 3000 rpm is shown in Fig. 3. For a given rotating speed, one can see that the current increases as the voltage is increased. It then reaches a plateau where diffusion becomes the rate-limiting step. The current at the plateau is called the limiting current, i_l. Values of limiting currents determined from these voltammograms were used to obtain the electrokinetic parameters of hydrogen oxidation.

For a simple electrode process, such as the hydrogen oxidation at a platinum–potassium hydroxide interface, the current-over potential relation can be obtained from the Butler–Volmer equation [18]. By neglecting the cathodic term, one can write

$$i = -i_0\left(\frac{C_{x=0}}{C_0}\right)\exp\left(\frac{\eta}{g_a}\right) \quad (1)$$

where i_0 is the exchange current density, $C_{x=0}$ the concentration of the species (i.e. hydrogen) at the electrode surface, C_0 the concentration of species in the bulk of the solution. The concentration ratio term can be estimated from the following expression [18]

$$\left(\frac{C_{x=0}}{C_0}\right) = 1 + \frac{i}{i_l} \quad (2)$$

where i_l is the limiting current and i is the anodic current which is negative.

By substituting Eq. (2) into Eq. (1) one obtains the mass transfer-corrected expression for an anodic reaction

$$\ln\left[\frac{ii_l}{(i_l - i)}\right] = \ln(i_0) + \frac{\eta}{g_a} \quad (3)$$

Tafel slopes and exchange current densities are directly obtained from the slopes and intercepts of the current–potential curves. In a typical mass transferred corrected plot, see Fig. 4, only one well-defined linear region can be seen and it is usually valid for an over-potential range of 50 to 200 mV. Table 1 shows the electrokinetic parameters of hydrogen oxidation at a platinum–potassium hydroxide interface determined by the above procedure. The values for the electrokinetic parameters of oxygen reduction at a platinum–

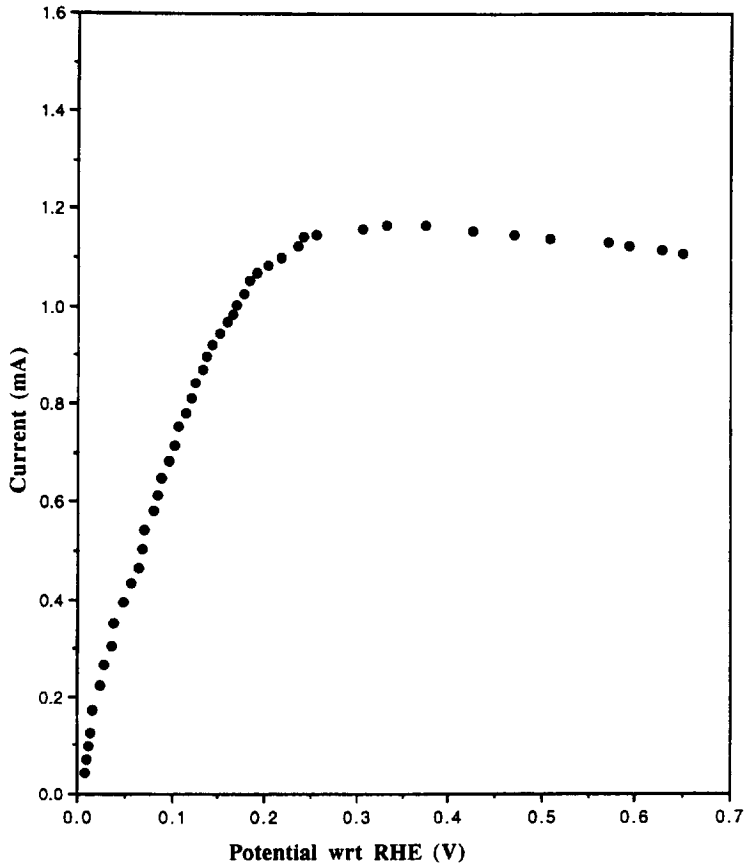

Fig. 3. Typical voltammogram for hydrogen oxidation on a platinum electrode at 3000 rpm, 0.1 N KOH and 65 °C.

Table 1
Electrokinetic parameters of hydrogen oxidation at a platinum–potassium hydroxide interface for different temperatures and concentrations

KOH	45 °C		65 °C		80 °C	
(N)	g_a (V)	$i_{0,a}$ (mA/cm^2)	g_a (V)	$i_{0,a}$ (mA/cm^2)	g_a (V)	$i_{0,a}$ (mA/cm^2)
0.1	0.046	1.884	0.041	4.077	0.052	2.960
0.5	0.052	1.573	0.060	1.542	0.042	5.263
6.0	0.043	0.259	0.043	0.463	0.075	0.737

Table 2
Electrokinetic parameters of oxygen reduction at a platinum–potassium hydroxide interface for different temperatures and concentrations [15]

KOH	45 °C		65 °C	
(N)	g_c (V)	$i_{0,c}$ (nA/cm^2)	g_c (V)	$i_{0,c}$ (nA/cm^2)
0.1	0.030	0.567	0.031	0.629
0.5	0.025	0.259	0.029	1.100
6.0	0.027	2.150	0.030	4.440

potassium hydroxide interface reported in a previous study [15] are shown in Table 2. The results in Table 1 indicate that in general the exchange current density decreases as the basicity of the KOH solution increases except, at 80 °C and 6.0 N. In general, the exchange current increases as the temperature increases except at 80 °C and 0.5 N. Tafel slopes show little change over a wide range of concentrations and temperatures except at high concentration and temperature (80 °C and 6.0 N).

3.2. Fuel cell electrode studies

The potential–current density curves obtained from electrodes with 10, 19 and 29 mg/cm^2 of nickel were obtained. A typical set of curves is shown in Fig. 5. The current–potential curves of the electrodes with a nickel film of 10 mg/cm^2 showed that the effect of increasing the temperature of the cell from 26 to 62 °C is a decrease in polarization of approximately 33 mV at the cathode and 66 mV at the anode at a current density of 100 mA/cm^2. The internal resistance free voltage was about 871 and 19 mV at the cathode and anode, respectively. The experimental data also indicate that an internal resistance free cell voltage of 854 mV is possible if the same type of electrodes are used as the anode and cathode in a single fuel cell. The polarization became significant in the anode at about 500 mA/cm^2.

The experimental results for the electrodes with a nickel coating of 19 mg/cm^2 indicated that when the temperature is increased from 26 to 62 °C the polarization at 100 mA/cm^2 is decreased by 25 and 83 mV at the cathode and anode, respectively. At 62 °C the internal resistance free voltage at the above current density was 888 and 15 mV at the cathode

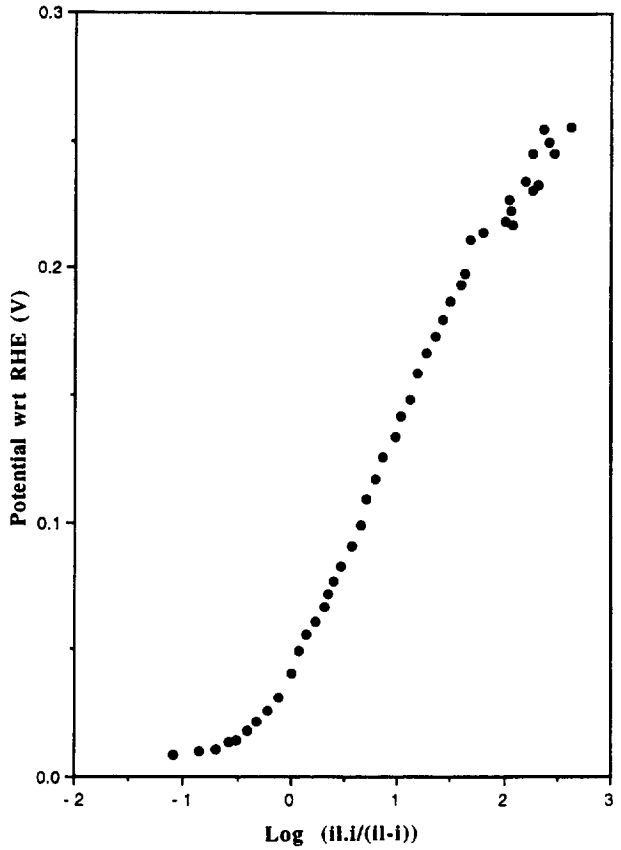

Fig. 4. Typical mass transferred corrected plot obtained from the rotating disk electrode measurements.

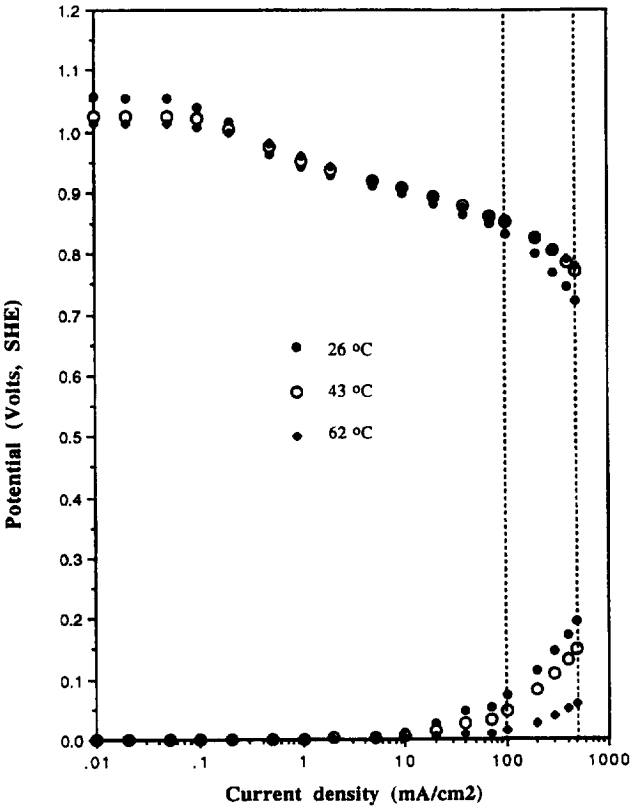

Fig. 5. Potential–current density curves of electrodes coated with 10 mg/cm^2 of nickel.

and anode, respectively. These results suggest that a possible terminal voltage of 873 mV can be achieved if the same type of electrode is used as anode and cathode in a fuel cell. Again the polarization started to be significant at a current density of 500 mA/cm^2.

The experimental results for the electrodes with a nickel coating of 29 mg/cm^2 indicated that at 100 mA/cm^2 the polarization is decreased by 13 and 80 mV at the cathode and anode, respectively, when the temperature was increased from 26 to 62 °C. The anode and cathode potential at 100 mA/cm^2 were 875 and 13 mV, respectively. These results indicate that at 62 °C a possible internal resistance free potential of 862 mV can be achieved for fuel cells using these type of electrodes.

The results indicate that the electrode performance improves with the increase in temperature. However, the temperature effect is larger in the electrodes working as anodes than when they are working as cathodes. This is attributed to the water production in the anode. This water can block the reaction sites in the electrodes. Increasing the cell temperature helps to remove the water being produced at the hydrogen electrode and consequently to improve the electrode performance. If one considers current densities below 100 mA/cm^2 the polarization problem seems to be at the cathode. However, above 100 mA/cm^2 the polarization starts to play a more significant role. At 500 mA/cm^2 the polarization at the anode increases greatly while at the cathode the polarization curve is still linear and the voltage sustained is about 800 mV.

The half-cell measurements indicated a consistent decrease in internal resistance as the thickness of the nickel coating increased (see Table 3). These measurements also indicated that the internal resistance decreased as the cell temperature was increased. This is attributed to the ohmic contribution of the electrolyte which decreases as the temperature increases [19]. There was a small effect on performance due to the differences in internal resistance produced by the nickelization of the electrodes. These internal resistance differences were not larger than 10 mΩ which would account for about 1 mV potential drop at 100 mA/cm^2. In this size range the loss or improvement of performance due to the ohmic drop was small. To examine the effect of the internal resistance on the fuel cell performance, larger electrodes with a geometrical surface area of 64 cm^2 were manufactured and assembled in single fuel cells.

Table 3
Measured internal resistance in mΩ for electrodes tested in the half-cell system ($A = 11$ cm^2)

Temperature	Amount of nickel per electrode surface area		
(°C)	9 mg/cm^2	18 mg/cm^2	31 mg/cm^2
62	22.1	22.4	12.2
43	25.0	23.2	13.8
26	32.4	27.4	17.5

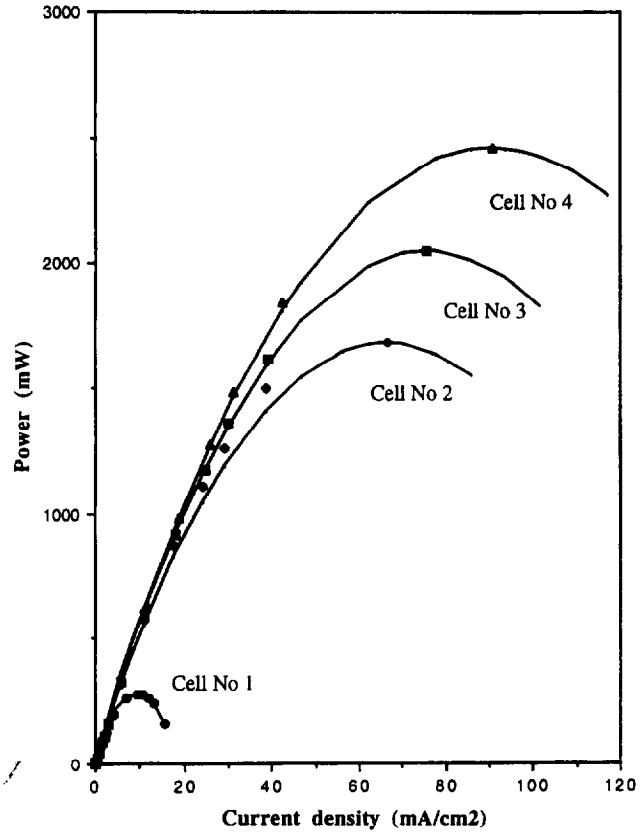

Fig. 6. Predicted and measured power output vs. current density of single fuel cells at 45 °C and 6.0 N KOH. Cell no. 1 had uncoated electrodes, cell no. 2 10 mg/cm^2 of nickel, cell no. 3 18 mg/cm^2 of nickel, and cell no. 4 25 mg/cm^2 of nickel. The predicted power output is represented by the solid line.

Four single fuel cells with different nickel coatings were assembled. One cell had uncoated carbon electrodes (cell no. 1) and the rest of the cells had a nickel coating of 10 mg/cm^2 (cell no. 2), 18 mg/cm^2 (cell no. 3), and 25 mg/cm^2 (cell no. 4). Potential, V and total current, I, measurements which corresponded to different loadings, R_l, were measured for the different fuel cells. From these measurements the power output as well as the current density were calculated. The power–current density curves of all single fuel cells at 45 °C are shown in Fig. 6. The internal resistance measurements for the single cells were 665.0, 86.3, 66.1 and 54.0 mΩ, respectively, and the corresponding maximum power outputs were 280, 1675, 2037 and 2444 mW, respectively. These results strongly indicate that the performance of a fuel cell can be significantly affected by its internal resistance which becomes a very important design parameter.

3.3. Internal resistance

The power produced by the fuel cell, P, may be written as [14]

$$P = I(V_e - V_p(I) - IR_i) \quad (4)$$

where V_e is the potential drop across the cell under open-circuit conditions, I the current, R_i the internal resistance, and V_p the kinetic and mass transfer polarization in terms of the current [14]

$$V_p(I) = g_a \ln\left(\frac{I}{e_f A_t i_{0a}}\right) + g_c \ln\left(\frac{I}{e_f A_t i_{0c}}\right) \quad (5)$$

where i_{0a} and i_{0c} are the equilibrium exchange current densities for the anode and cathode, respectively; e_f is the fraction of the electrocatalyst that is used effectively, and A_t is the total surface area of the catalyst in the cathode and anode, respectively. The experimental internal resistance was measured using the current interrupt technique [19]. Table 4 shows the experimental and predicted internal resistance for the single fuel cells tested in this study. It was observed that the internal resistance decreased significantly when the electrodes were nickel coated. Nickel coating the electrodes with 10, 18 and 25 mg/cm^2 decreased the internal resistance by 7.7, 10.1 and 12.3 times, respectively, when compared with the uncoated electrodes. The contribution of the electrolyte to the internal resistance measurements was estimated and found to be negligible. The specific conductance of KOH at 20 °C is 128 Ω^{-1} cm^{-1}. It was estimated that the electrical resistance for an electrode separation of 1.8 mm and a surface area of 64 cm^2 is 2.2×10^{-5} Ω which is at least three orders of magnitude below the values obtained from the current interrupt measurements.

An expression of the internal resistance in terms of the electrokinetic parameters and the maximum power condition has been reported [14]. This expression is in terms of the Tafel slope and the voltage (V_m) and current (I_m) at maximum power condition

Table 4
Comparison of calculated and measured internal resistance and effective catalyst fraction for different single fuel cells. The temperature for measurements and calculations was 45 °C. The electrolyte concentration was 6.0 N. The geometrical surface area of the catalyst was 1.79×10^4 cm^2

Cell nos.	Nickel coating (mg/cm^2)	R_i IT (mΩ)	R_i MP (mΩ)	$R_{i,a}$ AMP (mΩ)	e_f MP (%)	$e_{f,a}$ AMP (%)	I_m (A)	V_m (V)
1	0	665 ± 9.7	654.0	650.0	5.4	5.1	0.603	0.464
2	9	86.3 ± 2.6	76.3	86.8	5.1	10.6	4.252	0.3941
3	18	66.1 ± 6.9	72.2	71.2	12.2	11.9	4.850	0.420
4	31	54.0 ± 1.3	60.5	57.9	15.1	13.2	5.805	0.421

[a] IT: interrupt technique, MP: maximum power method, and AMP: 'approximate maximum power method'.

$$R_i = \frac{V_m - g_a - g_c}{I_m} \quad (6)$$

Since the electrokinetic parameters, the voltage and the current at maximum power are known, the electrokinetic parameters can be examined by comparing the measured internal resistance and the predicted internal resistance from Eq. (6). These values are reported in Table 4. By comparing both the predicted and experimental values of internal resistance, a difference within 12% of each other was found. These results suggested that the proposed 'maximum power method' predicts the internal resistance of the fuel cell within the above experimental error.

The expression of the internal resistance using the 'approximate maximum power method' reported in Ref. [14] was

$$R_{ia} = \frac{\sigma_0(2g_a + 2g_c + I_0\sigma_0 - V_0)}{V_0 - I_0\sigma_0} \quad (7)$$

where I_0, V_0 and σ_0 are the current, voltage and slope of the V–I relation to be measured at a condition where the current is less than that corresponding to the maximum power condition. The above expression was used to estimate the internal resistance for cells nos. 1, 2, 3 and 4, respectively. The value of the approximate current used for the calculations was 90% of the maximum current in each case. The predicted and measured values are summarized in Table 4. (Notice the good agreement between the approximate and maximum power method for all the evaluated fuel cells.) The approximate method may be a good alternative in situations where the fuel cell cannot be operated at maximum power under steady-state conditions (because of overheating problems).

3.4. Fraction of catalyst area used effectively

An expression of the fraction of the effective catalyst area has been recently reported [14]. This expression is in terms of the electrokinetic parameters (Tafel slopes and exchange current densities) and the two parameters that may be measured directly when the fuel cell is operating at maximum power: (i) the voltage, and (ii) the current

$$e_f = \exp\left[\frac{g_a \ln\left(\frac{I_m}{A_t i_{0a}}\right) + g_a \ln\left(\frac{I_m}{A_t i_{0c}}\right) + 2V_m - g_a - g_c - V_e}{(g_a + g_c)}\right] \quad (8)$$

Eq. (8) was used to estimate the fraction of the platinum area being used effectively in single fuel cells. It was found that cells nos. 1, 2, 3 and 4 were using 5.8, 5.1, 13.3 and 16.4% of the total catalyst area, respectively. (Notice that as the thickness of the nickel coating of the electrodes was increased, the fraction of the catalyst used effectively increased by a factor of three.) One possible explanation for this result is that the nickel coating the electrodes increases the charge (electrons) flow which is translated into a better electrocatalyst utilization. The fact that only a fraction of the catalyst layer is available for the electrochemical reactions (within 5 to 16.4%) means that in this process of electrode manufacturing most of the catalyst is not used effectively. The reason is that the platinum spheres deposited on the electrode are partially covered by the Teflon™ and carbon particles which are in the surrounding area of the platinum particles. Also part of the electrode is immersed in the electrolyte and part of it in the gas side is dry [4].

Theoretical and experimental curves of the four fuel cells tested in this study are shown in Fig. 6. In each case a theoretical curve was obtained from Eq. (4). The current and voltage at maximum power from experimental measurements were used to determine the internal resistance and the fraction of the catalyst area being used effectively. Then these parameters were used to predict all the other points in the measured power–current curves. (Note that the 'maximum power method' was used successfully in describing the experimental results at 45 °C and 6.0 N. The good agreement between the predicted and experimental values indicates the validity of the measured electrokinetic parameters.

Also an expression of the fraction of the catalyst used effectively obtained from the 'approximate maximum power method' that does not require the current and voltage at maximum power condition has been reported [14]

$$e_{fa} = \exp\left[\frac{V_0 - V_c - I_0\sigma_0 - g_a - g_c + g_a \ln\left[\frac{\sigma_0 I_0 - V_0}{2\sigma_0 A_t i_{0a}}\right] + g_c \ln\left[\frac{\sigma_0 I_0 - V_0}{2\sigma_0 A_t i_{0c}}\right]}{g_a + g_c}\right] \quad (9)$$

The predicted values of the effective catalyst fraction were estimated using Eq. (9) for cells nos. 1, 2, 3 and 4, respectively. The approximate current used was 90% of the maximum current. To obtain the slope and approximate voltage a logarithmic based curve was fit to the measured data points. The predicted values are summarized in Table 4. (Notice the close agreement between the predicted values from the 'approximate maximum power method' and those estimated from the 'maximum power method' for cells nos. 1, 2 and 3, respectively. For fuel cell no. 2 the fraction predicted using the approximate method was twice that from the maximum power method. The reason for this discrepancy is that the prediction of the catalyst fraction from the 'approximate maximum power method' is very sensitive to the measured slope at the approximate current value used in Eq. (9). (Notice the exponential dependence of the effective catalyst fraction with respect to the measured appproximate slope.) Since we did not have sufficient measured points in the region of the considered approximate current the slope was estimated from a best curve fit, logarithmic based, to the experimental measurements.

4. Conclusions

The rotating disk measurements for the platinum–potassium hydroxide interface indicated that, in general, the

exchange current density decreases for higher concentrations of potassium hydroxide and increases for higher temperatures. However, the Tafel slope shows little change over a wide range of KOH concentrations and different temperatures except at both high concentration and temperature.

The effect of increasing the temperature from 26 to 62 °C was greater in the nickel coated electrodes working as anodes than in the those working as cathodes. The major polarization problem in these electrodes below a current density of 100 mA/cm^2 was at the cathode. The polarization for current densities around 500 mA/cm^2 was larger at the anode. Nickel coating the carbon electrodes helped to reduce their ohmic resistance which is a very important contribution to the total internal resistance of the fuel cell. By depositing the amount of nickel of 10, 18 and 25 mg/cm^2 the internal resistance of the single fuel cells was reduced 7.7, 10.1 and 12.3 times, respectively, when compared with the fuel cell with uncoated electrodes.

Predictions from both mathematical methods, 'maximum power' and 'approximate maximum power method', were in reasonable agreement with measurements of performance and internal resistance of alkaline fuel cells with platinized-porous carbon electrodes. These methods are applicable to fuel cells limited by activation and ohmic polarization only. The good agreement between the experimental and predicted performance of the single fuel cells at 45 °C and 6.0 N indicates the validity of the measured electrokinetic parameters. The internal resistances determined by the current interrupt technique and those determined by the 'maximum power method' were within the maximum of 12% of each other for the single fuel cells examined in this study. The range of catalyst fraction used effectively determined by the proposed methods was from 5 to 16.4% for the examined fuel cells, an increase of the electrocatalyst utilization by a factor of three. This result is attributed to an improved release of charge by the deposited nickel layer.

The nickel coated electrodes developed in this work may be an attractive alternative where light weight and low internal resistance is required. The internal resistance was identified as an important design parameter and these results suggested that the fuel cell performance can be improved by modifying its design.

References

[1] R.R. Paxton, J.F. Demendi, G.J. Young and R.B. Rozelle, *J. Electrochem. Soc., 110* (1963) 932.
[2] A.J. Salkind, H.J. Canning and M.L. Block, *Electrochem. Technol., 2* (1964) 254.
[3] A. Pebbler, *J. Electrochem. Soc., 133* (1986) 9.
[4] L. Pataki, R.D. Venter and D. McCammond, *Proc. 5th Hydrogen Energy Conf., Toronto, Canada,* Pergamon, Oxford, Proc. Vol. 4, 1984, pp. 1831–1838.
[5] A.K. Shuckla, K.V. Ramesh, R. Manoharan, P.R. Sarode and S. Vasudevan, *Ber. Bunsenges. Phys. Chem 89* (1985) 1261.
[6] L.T. Wolf and G. Wilemski, *J. Electrochem. Soc., 130* (1983) 48.
[7] G. Wilemski, *J. Electrochem. Soc., 130* (1983) 117.
[8] V. Sampath and A.F. Sammells, *J. Electrochem. Soc., 127* (1980) 79.
[9] R.P. Iczkowski and M.B. Cutlip, *J. Electrochem. Soc., 127* (1980) 1433.
[10] S.C. Yang, M.B. Cutlip and P. Stonehart, *Electrochim. Acta, 35* (1990) 869.
[11] M.C. Kimble and R.E. White, *J. Electrochem. Soc., 138* (1991) 3370.
[12] M.C. Kimble, and R.E. White, *J. Electrochem. Soc., 139* (1992) 478.
[13] J. O'M. Bockris and B.D. Cahan, *J. Chem. Phys., 50* (1969) 1307.
[14] C.A. Ward and J.A. Garcia, J. Power Sources, (1996) submitted for publication.
[15] S.-M Park, S. Ho, S.A. Aruliah, M.F. Weber, C.A. Ward, R.D. Venter and S. Srinivasan, *J. Electrochem. Soc.*, 133 (1985) 1641–1649.
[16] M. Weber, S. Mamiche-Afara, M. Digman, L. Pataki and R.D. Venter, *J. Electrochem. Soc.*, 134 (1987) 1416.
[17] A. Tvarusko, *J. Electrochem. Soc.*, 109 (1962) 557.
[18] J. O'M. Bockris and A.N.K. Reddy, *Modern Electrochemistry*, Plenum, New York, 1973, p. 1371.
[19] A. Hickling, *Trans. Faraday. Soc., 33* (1937) 1540.